SIMILITUDE CONSIDERATIONS IN NEUTRON AND GAMMA RAY SCATTERING

Kenneth C. Ney

Library
U. S. Naval Postgraduate School
Monterey, California

[illegible]
[illegible]

[illegible]

[illegible]

[illegible]
[illegible]
8P [illegible]
[illegible]

[illegible]

[illegible]

[illegible]

[illegible]

[illegible]

[illegible]
[illegible]

SIMILITUDE CONSIDERATIONS IN NEUTRON
AND GAMMA RAY SCATTERING

by

Kenneth C. Moy

A Thesis Submitted to the
Graduate Faculty in Partial Fulfillment of
The Requirements for the Degree of
MASTER OF SCIENCE

Major Subject: Nuclear Engineering

TABLE OF CONTENTS

Page

I. INTRODUCTION 1

II. REVIEW OF LITERATURE 2

III. SCOPE OF INVESTIGATION 4

IV. THEORETICAL ANALYSIS 5

A. Assumptions 5
B. Neutron Scattering 10
C. Gamma Ray Scattering 27

V. EXPERIMENTAL PROGRAM 32

A. Materials 32
B. Equipment 33
C. Procedure 37

VI. EXPERIMENTAL RESULTS AND DISCUSSION 43

A. Neutron Scattering 43
B. Gamma Ray Scattering 47
C. General Discussion 50

VII. CONCLUSIONS 52

VIII. LITERATURE CITED 53

IX. ACKNOWLEDGMENTS 54

X. APPENDIX 55

A. Sample Analytical Computations 55

28889

I. INTRODUCTION

The current development of nuclear powered aircraft involves many problems which are relatively unimportant in the design of large permanently located reactors. One of these problems is the design of shielding arrangements which will materially reduce the weight of the shield and yet sufficiently protect the crew. One possibility is the use of a shadow shield between the reactor and the crew compartment. Another is a split shield where the shielding placed next to the reactor reduces the radiation to some degree and additional shielding placed around the crew compartment reduces the radiation within the compartment to permissible levels.

With shielding arrangements of these or similar types some of the reactor-produced neutron and gamma-ray radiation will be scattered by the structure of the aircraft. To design the shield properly, the amount of this scattered radiation that enters the crew compartment must be found. This can either be done by mathematical or direct measurement methods. Considering the complex structure that an airplane necessarily has, the latter method employing a model of the airplane is probably the more feasible way.

Thus, the relationship between the scattering by the model and the full-scale structure must be known. This relationship with a simplified structure was the object of this investigation.

II. REVIEW OF LITERATURE

No investigations on the subject of similitude considerations in the scattering of neutrons and gamma rays by structural material were found in the literature. However, many studies related to this subject are available.

Glasgow (1) investigated the scattering of neutrons from the walls and air of a laboratory by suspending from the center of the ceiling a source and detector at various distances above the floor of a cubic room. The expressions he used for calculating the expected scattering were for an infinite air medium and for the flux of scattered neutrons returning to a source when the source is midway between two non-capturing semi-infinite media, here the walls.

Plesset (2) developed formulas for the intensity of gamma rays scattered by air from a source to a receiver but restricted his analysis to single scattering. He made similar calculations for the intensity of neutrons singly scattered by air from a source to a receiver. He also developed approximate expressions for the reflection of gamma rays and neutrons from a semi-infinite slab.

As a continuation of this, Plesset and others (3) illustrated by exact calculations the geometrical effects of the size of a shadow shield and a source on the intensity of gamma rays scattered into a receiver.

The gamma ray backscattering from various materials was investigated experimentally and qualitatively by Hine and McCall (4). The experimental procedure involved placing a point source on or having it suspended over

the horizontally placed scattering material with a NaI(Tl) crystal detector placed vertically above the source. The results were plotted to show the relationship between the scattered gamma rays and the energy of the primary gamma radiation for the various geometries used.

Plesset and Cohen (5) presented formulas for the calculation of the differential cross section $d\sigma/d\Omega$ for the scattering of gamma rays into an element of solid angle and gave a graph of $d\sigma/d\Omega$ versus the angle of scatter. Also, the development of an expression for the intensity of the gamma radiation at a point in an infinite medium due to the direct radiation and scattered radiation was given.

All of these investigations were made with point receivers and with what can be considered infinite or semi-infinite scattering media. In the problem investigated in this thesis detectors of finite size were used as the receivers and thin cylindrical shells were used as the scattering medium, thus, these related investigations could be used only as references and occasional guides.

III. SCOPE OF INVESTIGATION

The scattering of neutrons and gamma rays by thin cylindrical shells was investigated analytically and an attempt was made to verify these results by experimental means. The analytical investigation was made for point sources of radiation and finite size detectors, with the source positioned vertically below the center of the detector and with the center line of the detector coincident with the center line of the cylindrical shell.

Experimentally, the scattering of neutrons and gamma rays by 24ST and Alclad 24ST aluminum alloy cylindrical shells was investigated. However, the experimental results were overshadowed by the relatively large statistical deviations that were introduced when correcting the experimental readings for the scattering of the radiation by the air and the room.

Attempts to reduce this extraneous scattering to an acceptable level were unsuccessful. Thus, the experimental results with the exception of a few of the gamma ray readings neither proved or disproved the analytical findings. The few exceptions noted only tended toward support of the analytical results and no positive conclusions could be drawn.

IV. THEORETICAL ANALYSIS

A. Assumptions

The theoretical analysis of this problem concerning similitude in neutron and gamma ray scattering would have been extremely complicated without certain simplifying assumptions. These included the following.

It was assumed that the sources of radiation were point sources and that the neutrons or gamma rays were emitted isotropically. This is a valid assumption for very small finite sources. If the finite source cannot be considered very small, but is still small compared to the size of the scattering material, it can be approximated by a series of point sources.

Any scattering or absorption of neutrons or attenuation of gamma rays by the air was assumed to be negligible. That this is a valid assumption for neutrons follows from the magnitude of the probability that a neutron will be scattered or absorbed in air. The probability that a neutron will penetrate the air or other material a distance x without being scattered or absorbed is $e^{-\Sigma x}$ where Σ is the macroscopic cross section for the event in question.

For a substance composed of more than one element Σ is calculated by using the formula

$$\Sigma = \rho N \sum_i \frac{f_i \sigma_i}{A_i} \qquad (1)$$

where ρ is the density of the substance

N is Avogadro's number

f_i is the weight fraction of the ith element of the substance

σ_i is the microscopic cross section of the ith element for the event in question

A_i is the atomic weight of the ith element.

For air at standard conditions, the value of Σ_s (scattering cross section) as calculated with this equation is 4.5×10^{-4} cm.$^{-1}$ and the value of Σ_a (absorption cross section) is 7.2×10^{-5} cm.$^{-1}$.

The maximum neutron path length from the source to the detector in this experiment was approximately 65 cm. Thus, the probability that a neutron would be scattered by the air in this experiment was about 0.03 for the maximum distance and considerably less than this for the minimum distance. The probability that a neutron would be absorbed was approximately 0.005 for the maximum distance. These probabilities are for thermal neutrons. As the neutron energy increases Σ_s remains about constant and Σ_a is reduced considerably, so the absorption probability will be less than 0.005 for higher energy neutrons.

That the attenuation of gamma rays by air is very small can be seen by applying the factor $e^{-\mu x}$ which is the probability that a gamma ray will penetrate a distance x into a medium without being involved in any reaction that contributes to its attenuation. The total absorption coefficient μ is the sum of the absorption coefficients for photoelectric effect, Compton scattering, and pair production. For air, μ

varies between approximately 1×10^{-4} cm.$^{-1}$ for 0.5 Mev gamma rays and 0.40×10^{-4} cm.$^{-1}$ for 4 Mev gamma rays (5). Therefore, the probability that a gamma ray within this energy range would be attenuated by the air was about 0.0065 to 0.0026 for the maximum distance involved in this experiment.

Another assumption used concerned the number of scattering collisions undergone by each neutron in the 24ST aluminum or Alclad 24ST aluminum cylindrical shells. It was assumed that each neutron that was scattered was involved in only one scattering collision. A consideration of the mean free path for neutron scattering λ_s in 24ST aluminum alloy or Alclad 24ST aluminum alloy shows that this assumption is valid. The mean free path λ_s is equal to $1/\Sigma_s$. Equation (1) was evaluated to find Σ_s.

The density of 24ST wrought aluminum alloy is 2.77 grams per cubic cm. and its nominal composition (6) is 4.5 per cent copper, 0.6 per cent manganese, 1.5 per cent magnesium, and 93.4 per cent aluminum with its normal impurities. These normal impurities and the permissible maximum of each are 0.5 per cent iron, 0.5 per cent silicon, 0.1 per cent zinc, and 0.1 per cent chromium. The cladding material, which is nominally 5 per cent of the total thickness of sheet 0.064 inch or over in thickness and 10 per cent for sheet less than 0.064 inch thickness, has a density of 2.71 grams per cubic cm. Its nominal composition is 99.3 per cent minimum aluminum with impurities of 0.7 per cent maximum iron plus silicon, 0.1 per cent maximum copper, 0.1 per cent maximum zinc, and 0.05 per cent maximum manganese.

Assuming that the amount of the impurities present is one-half

[illegible]

[illegible]

[illegible]

[illegible]

of the maxima, Σ_s for thermal neutrons for this alloy is 0.0943 cm.$^{-1}$ and Σ_s for the cladding is 0.085 cm.$^{-1}$. Thus λ_s, which like Σ_s remains approximately constant with increasing neutron energy, is 10.6 cm. for the alloy and 11.76 cm. for the cladding. These values when compared with the maximum effective thickness of the material considered in this experiment, which is about 0.62 cm., show that the assumption of only one collision for each neutron scattered should not have introduced any great error.

This scattering was assumed to be spherically symmetrical which would only be true if the mass of the scattering nucleus was much larger than the mass of the neutron. A measure of the anisotropy of the neutron scattering is the average cosine of the scattering angle in the laboratory system. Glasstone and Edlund (7, p. 97) showed that this average cosine for neutrons with energies less than a few Mev is given by the equation

$$\overline{\cos\ \psi} = \frac{2}{3A}$$

where A is the mass number of the scattering material. The mass number of 24S aluminum alloy, which is the sum of the weighted mass numbers of the constituents, is 28.89. The mass number of the cladding computed in a similar manner is 27.10. Thus, $\overline{\cos\ \psi}$ is 0.0231 for the alloy and 0.0246 for the cladding which indicates that the anisotropy is relatively low.

The slowing down of fast neutrons is due almost entirely to

elastic scattering of the neutrons upon collision with nuclei of the moderator, therefore, it was assumed that all the collisions in the scattering material were elastic.

Throughout the entire development, the absorption cross section was assumed to be small compared with the scattering cross section. Actually, since the absorption cross section for most elements decreases fairly rapidly with increasing neutron energy, this assumption would be of little concern in the designing of shielding that must protect personnel from structurally scattered neutrons. Any shield that would protect them from fast neutrons would be effective against slow neutrons. Therefore, only calculations for fast neutron scattering would be necessary and in this energy range the absorption cross section is, with few exceptions, much smaller than the scattering cross section.

If for some reason the number of scattered slow neutrons must be known, this can be estimated quite accurately by slightly modifying the equation developed for fast neutrons. This modification is given at the end of the development of the fast neutron scattering equation.

The mean free path for neutron scattering λ_s is actually a function of energy. If the source of neutrons is not monoenergetic, this introduces another variable. However, λ_s is practically a constant for neutrons up to about 8 or 10 Mev and, therefore, it was assumed that a constant value could be used for a polyenergetic source of neutrons.

The differential cross section $d\sigma/d\Omega$ for monoenergetic gamma ray scattering is a function of the angle of scattering. However, calculations show (5) that this is practically constant for angles of scattering greater than about 70 degrees. In this investigation, the angle of scattering, with few exceptions, was greater than this, thus a constant value was assumed for $d\sigma/d\Omega$.

B. Neutron Scattering

Figure 1 is a sketch of the system investigated. The scattering material comprises a cylindrical shell of radius r, thickness t, and height h_4, one-quarter of which is shown. The counting tube with an active volume of radius a and height h_2 and the point source are positioned on the center line of the cylindrical shell with the center line of the counting tube coincident with that of the shell. The top of the active volume of the vertically suspended counting tube is on the same horizontal level as the top edge of the scattering material. The point source is located on a horizontal line which is a distance h_3 from the top edge of the scattering material and a distance h_1 from the bottom edge.

The equation which gives the number of neutrons that are singly scattered by the cylindrical shell into the counting tube was developed as follows.

The neutron flux ϕ which reaches the element of volume at P a distance r_1 from the source (Figure 1) is

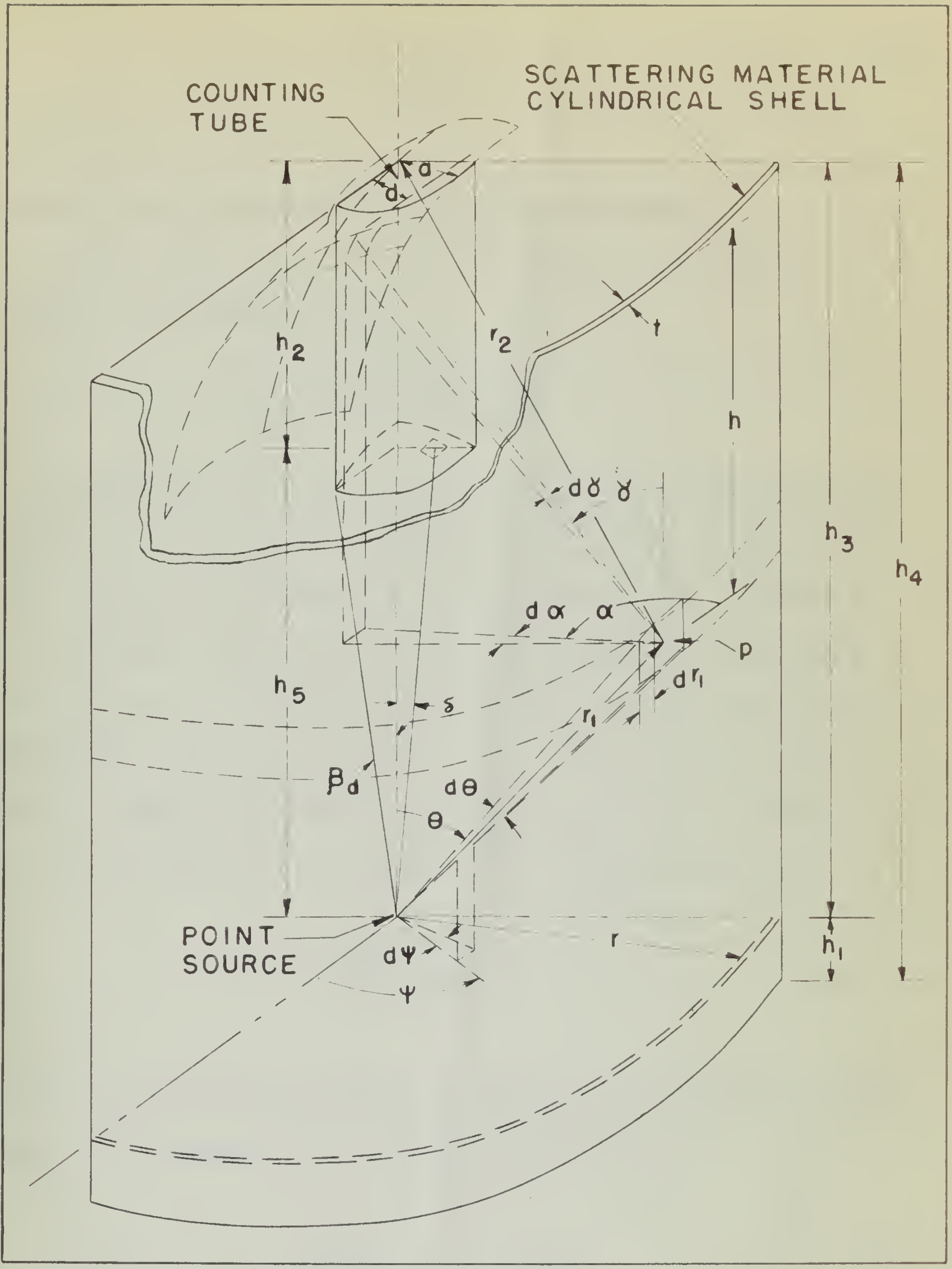
SCATTERING MATERIAL
CYLINDRICAL SHELL
COUNTING
TUBE
a
d
h_2
r_2
t
h
dγ
γ
h_3
h_4
dα
α
p
dr_1
h_5
δ
r_1
β_d
dθ
θ
POINT
SOURCE
dψ
ψ
r
h_1

Figure 1. Geometry of scattering.

$$\phi = \frac{Q}{4\pi r_1^2} \tag{2}$$

where Q is the source strength in neutrons per second.

The effective volume element at P normal to the path of a radially emitted neutron is

$$dV = r_1 \, d\Psi \, r_1 \, d\theta \, dr_1$$

A radially emitted neutron travels a distance dr_1 within this volume element. To determine the probability of a neutron being scattered while traveling this distance, the mean free path for scattering λ_s was used. This, the reciprocal of the macroscopic scattering cross section Σ_s, is the average distance a neutron travels between collisions. Thus, the probability that a neutron will be scattered while traveling the distance dr_1 is dr_1 / λ_s and the probability p that the neutron will be scattered within the volume element is

$$p = \frac{r_1^2 \, d\theta \, dr_1 \, d\Psi}{\lambda_s}$$

Therefore, the number of neutrons n which are singly scattered within this volume element, which is Equation (2) times p, is

$$dn = \frac{Q}{4\pi\lambda_s} \, d\theta \, dr_1 \, d\Psi \tag{3}$$

Assuming isotropic and elastic scattering, the proportion of the scattered neutrons that are scattered toward a point detector is $1/4\pi r_2^2$ where r_2 is the distance from the volume element to the point detector. However, with the geometry of the problem that was investigated here, the counting tube could not be regarded as a point detector. Instead, the ratio of the solid angle Ω subtended by the detector, as viewed from the element of volume, to the total solid angle of 4π steradians had to be used.

This solid angle can best be found by considering a spherical surface (see Figure 1) which passes through the center of the top of the counting tube and is generated by swinging an arc of radius r_2 centered at the volume element. Then by setting the proper limits on α and γ, the solid angle subtended by the counting tube can be determined.

The solid angle Ω is

$$\Omega = \int_{\alpha_1}^{\alpha_2} \int_{\gamma_1}^{\gamma_2} \sin \gamma \, d\gamma \, d\alpha \qquad (4)$$

where subscripts 1 and 2 signify, respectively, minimum and maximum.

The limits on α and γ are interdependent in a rather complicated way due to the shape of the counting tube. To avoid this complication and yet arrive at an equation which gives a good approximation of Ω, the limits on α are set at

$$\alpha_1 = \frac{\pi}{2} - \tan^{-1}\frac{a}{r}$$

$$\alpha_2 = \frac{\pi}{2} + \tan^{-1}\frac{a}{r}$$

These limits on α are independent of the other angles, thus, Equation (4) becomes upon integration over α and substitution of these limits

$$\Omega = 2\tan^{-1}\frac{a}{r}\int_{\gamma_1}^{\gamma_2}\sin\gamma \, d\gamma \qquad (5)$$

Setting the limits on γ was not as simple a task as it first appeared. For instance, if γ_1 is taken to be $\cot^{-1} r/h$, part of the upper extremities of the counting tube would be excluded from the solid angle. On the other hand, if γ_1 is taken to be $\cot^{-1} (r-a)/h$, the solid angle would include some volume outside the counting tube. The same reasoning would apply to γ_2 when h is less than h_2. When h is greater than h_2, a value of $\cot^{-1} (h-h_2)/r$ for γ_2 would not include all the bottom surface of the counting tube in the solid angle. As a compromise, the limits on γ were taken in two parts and were set by using the distance r minus d, where d is the mean integrated semichord. This is found from the equation

$$d = \frac{\int_{x=-a}^{x=a} \sqrt{a^2-x^2}\ dx}{2a}$$

Thus

$$d = \frac{\pi}{4} a$$

Then the limits are

$$\gamma_1 = \cot^{-1} \frac{h}{r-d} \qquad (\text{all } h) \qquad (6)$$

$$\gamma_{21} = \cot^{-1} \frac{h-h_2}{r-d} \qquad (h \leq h_2) \qquad (7)$$

$$\gamma_{22} = \cot^{-1} \frac{h-h_2}{r+d} \qquad (h \geq h_2) \qquad (8)$$

The contribution of the bottom of the detector to the solid angle is included by making the denominator of the latter limit r+d.

These limits on γ are independent of ψ, but are dependent on θ being related through h by the equation

$$h = h_3 - r \cot \theta \qquad (9)$$

Equation (5) gives the solid angle subtended by the counting tube. This divided by the total solid angle 4π steradians is the proportion of scattered neutrons that will pass through the counting tube volume.

The number of neutrons scattered within the volume element is given by Equation (3), thus, this times the above ratio is the number of neutrons n_s that are scattered into the counting tube by the volume element. So

$$\int_0^{n_s} dn_s = \int_V \frac{Q}{16\,\pi^2\,\lambda_s}\left[2\tan^{-1}\frac{a}{r}\int_{\gamma_1}^{\gamma_2}\sin\gamma\, d\gamma\right] d\theta\;\; dr_1\, d\psi$$

The limits on ψ are zero and 2π and the limits on r_1 are $r/\sin\theta$ and $(r+t)/\sin\theta$ where t is the perpendicular thickness of the scattering material. Integrating over r_1 and ψ and substituting the limits give

$$n_s = \frac{Qt}{8\pi\lambda_s}\int_{\theta_1}^{\theta_2}\left[2\tan^{-1}\frac{a}{r}\int_{\gamma_1}^{\gamma_2}\sin\gamma\;\, d\gamma\right]\frac{d\theta}{\sin\theta} \qquad (10)$$

Integrating in this equation over γ and substituting the limits (Equations (6), (7), and (8)) and then substituting for h from Equation (9) result in an extremely complicated and lengthly integral of θ. To arrive at a simpler but still a good approximate expression for n_s, the bracket of Equation (10) which is the integral equation for Ω was replaced by the average value of Ω. This average value is found as follows.

Equation (5) is integrated and the limits as given by Equations (6),

(7), and (8) are substituted. This gives

$$\Omega = 2 \tan^{-1} \frac{a}{r} \left[\frac{h_2 - h}{\sqrt{(h-h_2)^2 + (r-d)^2}} + \frac{h}{\sqrt{h^2 + (r-d)^2}} \right] \qquad (h \leq h_2) \tag{11}$$

$$\Omega = 2 \tan^{-1} \frac{a}{r} \left[\frac{h_2 - h}{\sqrt{(h-h_2)^2 + (r+d)^2}} + \frac{h}{\sqrt{h^2 + (r-d)^2}} \right] \qquad (h \geq h_2) \tag{12}$$

The values of Ω throughout the range of h are found for the geometry involved by assigning values to h, say n_0, n_1, n_2,......n_i...h_4. These values run from zero to h_4 (Figure 1) and are equally spaced, the distance between them being b. Then the average value of Ω, say $\bar{\Omega}$, is found from the equation

$$\bar{\Omega} = \frac{\displaystyle\sum_{i=0}^{i=(h_4/b)-1} \frac{\Omega_i + \Omega_{i+1}}{2}}{h_4/b} \tag{13}$$

Values of $\bar{\Omega}$ for the various geometries used in this investigation are plotted in Figure 2.

Using this average value of Ω, Equation (10) can be written

$$n_s = \frac{Q\,\bar{\Omega}}{8\,\pi\,\lambda_s} \int_{\theta_1}^{\theta_2} \frac{d\,\theta}{\sin\theta} \tag{14}$$

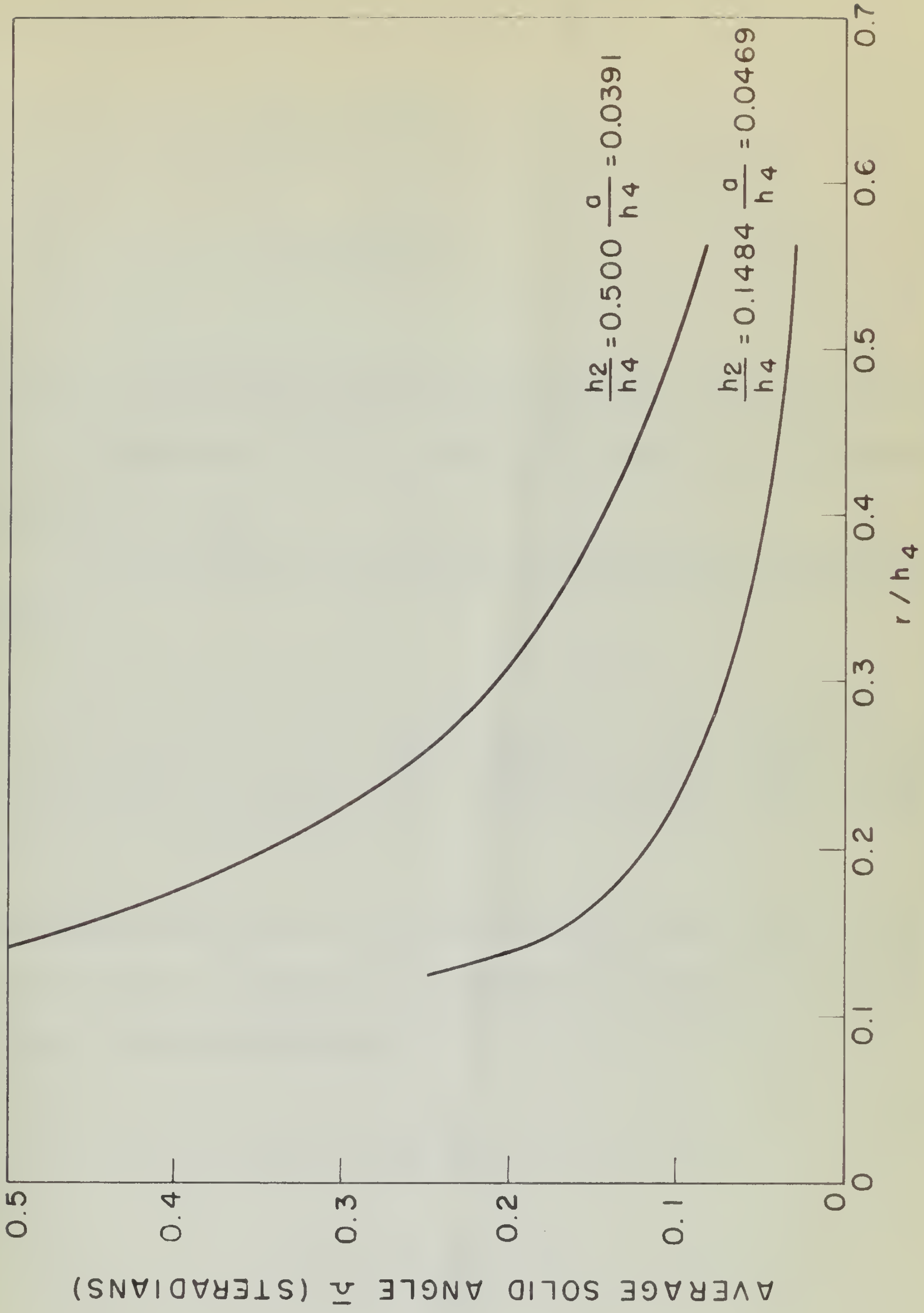

Figure 2. Average solid angle for various geometries.

From Figure 1, it is seen that the limits on θ are

$$\theta_1 = \cot^{-1} \frac{h_3}{r}$$

$$\theta_2 = \cot^{-1} \frac{h_1}{r}$$

where h_1 is considered positive if the bottom edge of the cylindrical shell is horizontally above the source and negative if the bottom edge is below the source.

The integration of equation (14) and substitution of the limits gives

$$n_s = \frac{Q \bar{\Omega} t}{8 \pi \lambda_s} \left[\ln \left(\sqrt{1 + \left(\frac{h_1}{r}\right)^2} - \frac{h_1}{r} \right) - \ln \left(\sqrt{1 + \left(\frac{h_3}{r}\right)^2} - \frac{h_3}{r} \right) \right]$$

Referring to Figure 1, it is evident that h_1/r is the tangent of the backward angle at the source and h_3/r is the tangent of the forward angle. Thus the substitution of

$$\tan \beta_b = \frac{h_1}{r}$$

$$\tan \beta_f = \frac{h_3}{r}$$

and combination of the natural log terms gives

$$n_s = \frac{Q \bar{\Omega} t}{8 \pi \lambda_s} \ln \left[\frac{\sqrt{1 + \tan^2\beta_b} - \tan\beta_b}{\sqrt{1 + \tan^2\beta_f} - \tan\beta_f} \right]$$

Now

$$\sqrt{1 + \tan^2\beta_b} = \frac{1}{\cos\beta_b}$$

and

$$\tan\beta_b = \frac{\sin\beta_b}{\cos\beta_b}$$

so that the numerator of the natural log in the above equation can be written $(1 - \sin\beta_b)/\cos\beta_b$. A similar expression can be substituted for the denominator to give

$$n_s = \frac{Q \bar{\Omega} t}{8 \pi \lambda_s} \ln \left[\left(\frac{1 - \sin\beta_b}{\cos\beta_b} \right) \left(\frac{\cos\beta_f}{1 - \sin\beta_f} \right) \right]$$

The final expression for n_s is found by letting

$$N = \ln \left[\left(\frac{1 - \sin\beta_b}{\cos\beta_b} \right) \left(\frac{\cos\beta_f}{1 - \sin\beta_f} \right) \right]$$

so that

$$n_s = \frac{Q\,\bar{\Omega}\,tH}{4\pi\lambda_s} \tag{15}$$

This equation gives the total number of neutrons per second that are singly scattered by the cylindrical shell into the counting tube volume. When evaluating H, it must be remembered that h_1 is considered positive if the bottom edge of the cylindrical shell is horizontally above the source and negative if the bottom edge is below the source. Therefore, β_b and, consequently, sin β_b are positive for the first mentioned conditions and negative for the latter. A plot of H versus β_b for various values of β_f is given in Figure 3.

For a polyenergetic neutron source, Equation (15) can represent the total number of fast neutrons that are singly scattered if Q is redefined as the fast neutrons per second emitted by the source. A possibility for the need of a slight modification to this equation arises from the fact that a small fraction of the fast neutrons emitted at energies just above thermal are reduced to thermal energies upon colliding with the nuclei of the structural material.

The energy E' of these neutrons after the collision is related to the energy E before the collision by the formula (7, p. 140)

$$E' = E\,\frac{A^2 + 2A\cos\epsilon + 1}{(A+1)^2}$$

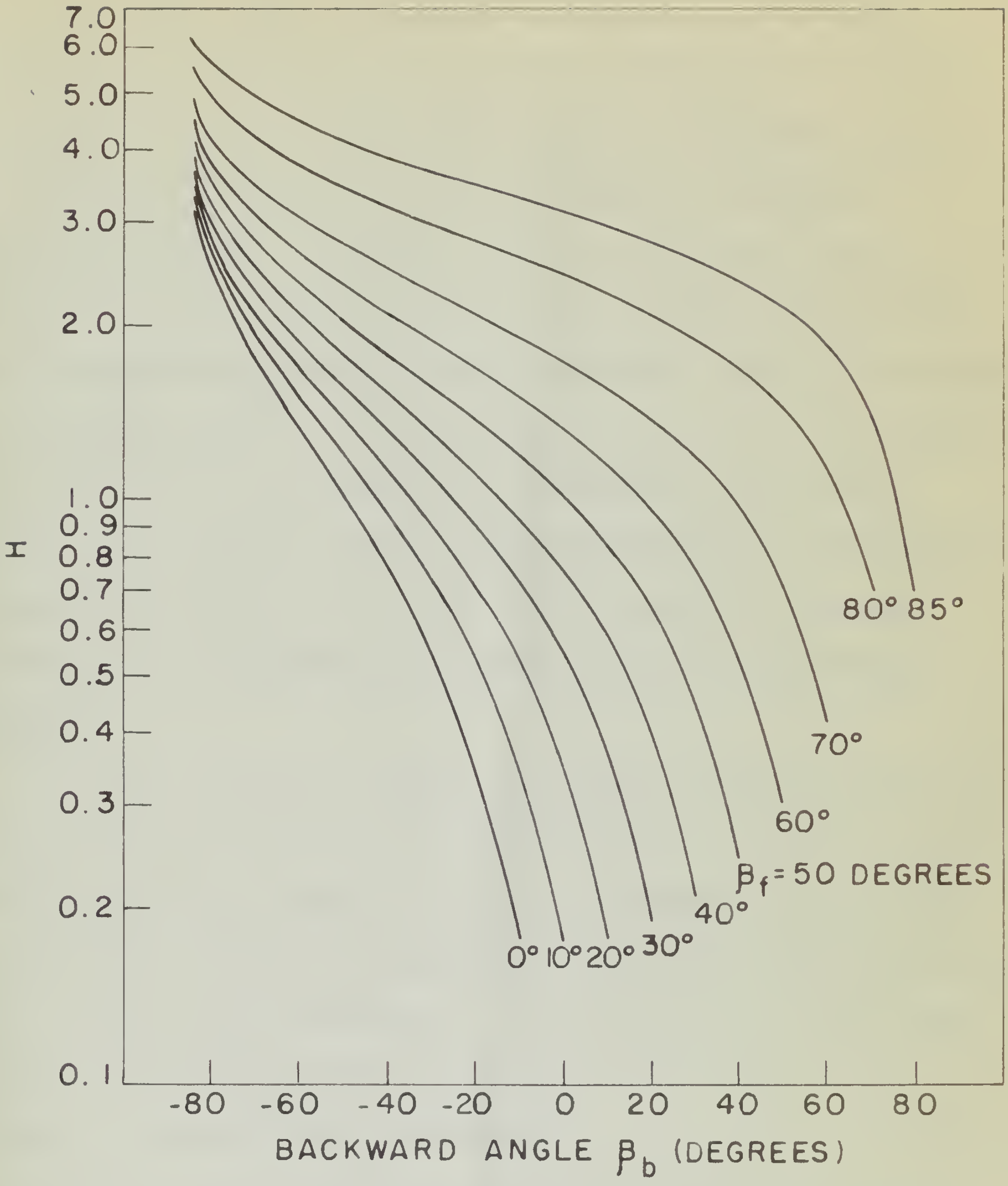

Figure 3. Variation of H with geometry.

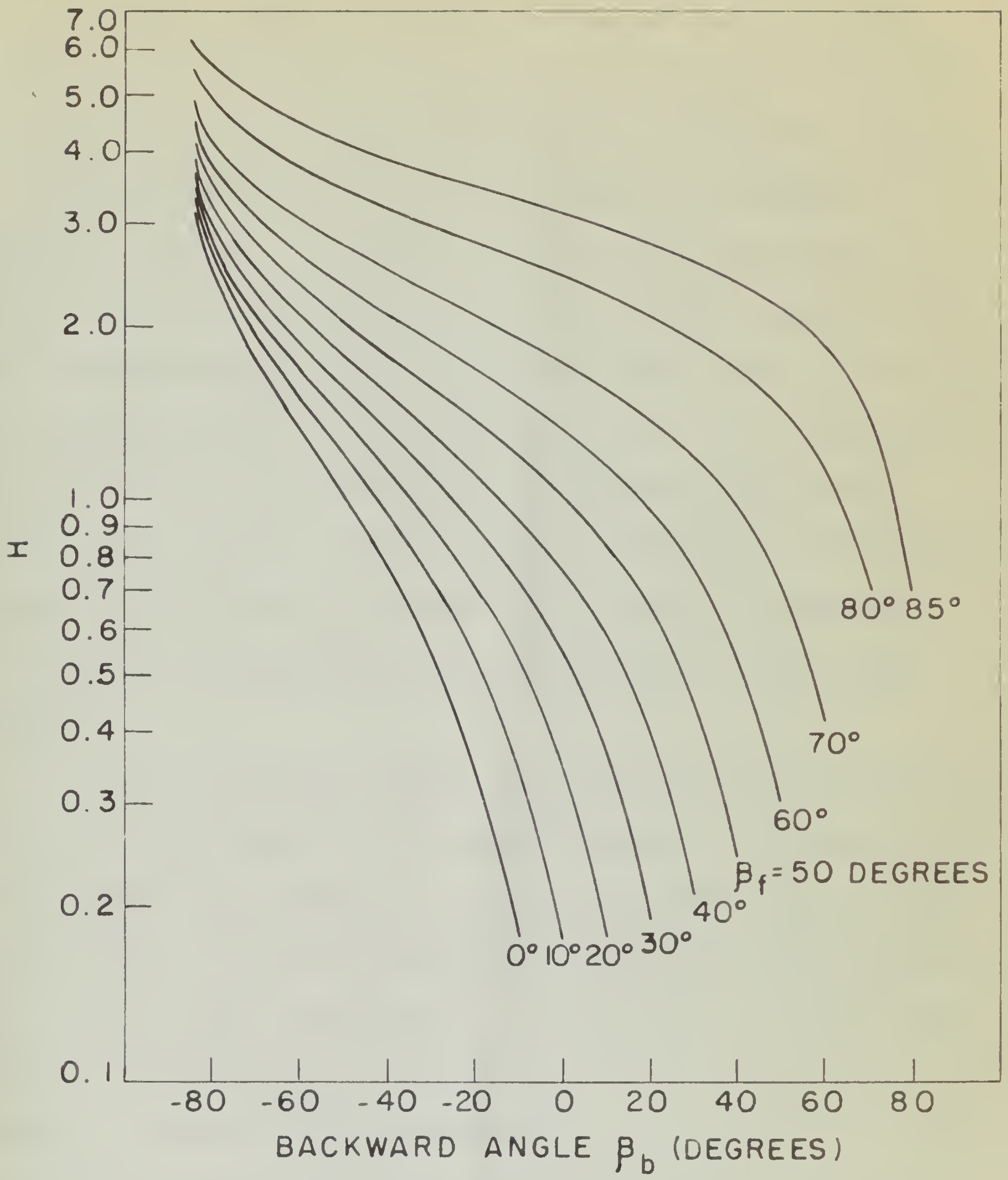

Figure 3. Variation of H with geometry.

where A is the mass number of the scattering material and ϵ is the scattering angle. Since the neutrons of interest here are those scattered into the thermal energy region, the energy after collision E' is E_t where E_t is the defined maximum energy of thermal neutrons.

In this investigation or in similar setups with shells of structural material, the scattering angle has an average value of about 90 degrees. For this scattering angle and 24ST aluminum alloy E', using the above equation, is equal to 0.935 E. Thus, on the average, those neutrons emitted by the polyenergetic source in the energy range from E_t to 1.07 E_t are scattered into the thermal neutron energy region. For example, if thermal neutrons are defined as those with an energy of 0.25 ev or less, the neutrons with energies between 0.25 and 0.268 ev are scattered upon collision into the thermal energy region.

For almost all neutron sources, the number of neutrons emitted in this very narrow energy band are a minute fraction of the total neutrons emitted. Hence, for practical purposes, all neutrons emitted as fast (slow) neutrons can still be considered as such after they are scattered. Thus, Equation (15) is applicable to fast neutrons, as are the subsequent equations given in this section, if Q is the number of fast neutrons per second emitted by the source.

Other measurements of the scattering by the cylindrical shells would be the ratio R_S of the neutrons scattered into the counting tube to those that reach the counting tube directly or the ratio R_T of the total neutrons that reach the counting tube to those that proceed

directly.

The number of neutrons that arrive directly is the point source strength Q times the ratio of the solid angle subtended by the end of the counting tube to the total solid angle 4π steradians. The solid angle subtended by the bottom of the quarter of the detector shown on Figure 1 is

$$\Omega = \frac{\pi}{2} \int_{\delta_1}^{\delta_2} \sin \delta \, d\delta$$

The limits on δ are zero and $\cot^{-1} h_5/a$, thus

$$\Omega = \frac{\pi}{2} \left(1 - \frac{h_5}{\sqrt{h_5^2 + a^2}} \right)$$

The solid angle Ω_d subtended by the bottom of the detector is four times this, or

$$\Omega_d = 2\pi \left(1 - \frac{h_5}{\sqrt{h_5^2 + a^2}} \right)$$

The proportion of the source neutrons which arrive directly at the detector is $\Omega_d/4\pi$, so the number n_d of source neutrons that arrive directly is

$$n_d = \frac{Q}{2} \left(1 - \frac{h_5}{\sqrt{h_5^2 + a^2}} \right)$$

The term in the parenthesis can be written as

$$1 - \frac{1}{\sqrt{1 + \left(\frac{a}{h_5} \right)^2}}$$

where (see Figure 1)

$$\frac{a}{h_5} = \tan \beta_d$$

Substituting from this relationship for a/h_5 and then substituting $1/\cos \beta_d$ for $\sqrt{1 + \tan^2 \beta_d}$ gives the final expression for n_d. Thus,

$$n_d = \frac{C}{2}(1 - \cos \beta_d) \qquad (16)$$

The scattering ratio R_S was previously defined as n_s/n_d (Equations (15) and (16)). So

$$R_S = \frac{\bar{\Omega}\, tN}{4\pi \lambda_s (1 - \cos \beta_d)} \qquad (17)$$

The total ratio R_T was previously defined as $(n_s + n_d)/n_d$ which equals $(n_s/n_d) + 1$. Thus

$$R_T = R_S + 1 \qquad (18)$$

Equations (17) and (18) can be applied to the total neutrons from a polyenergetic source or to the fast neutrons from a polyenergetic source or a monoenergetic source. These equations can also be applied to thermal neutrons if the cross section for absorption is negligible compared to the cross section for scattering. Under similar circum-

stances, Equation (15) can be used provided Q is the thermal neutrons per second emitted by the source.

If the absorption cross section is not negligible compared to the scattering cross section, but is still somewhat less than the scattering cross section and, if the thickness of the cylindrical shells used is small compared to the mean free path for absorption (which it must be for Equation (15) to be valid), a good first approximation of the thermal neutron scattering can be calculated as follows.

The fraction of normally incident thermal neutrons that would be absorbed in the shell, if the scattering cross section were negligible, is $(1 - e^{-\Sigma_a t})$ where Σ_a is the macroscopic absorption cross section and t is the thickness of the shell. This fraction times Equation (15) gives a good first approximation of the number n_{s_t} of thermal neutrons scattered by the cylindrical shell into the counting tube volume. Thus

$$n_{s_t} = \frac{Q\,\bar{\Omega}\,t\,l}{8\pi\lambda_s}\left(1 - e^{-\Sigma_a t}\right) \tag{19}$$

Equations (17) and (18) are, for this case,

$$R_{S_t} = \frac{n_{s_t}}{n_{d_t}} \tag{20}$$

and

$$R_{T_t} = R_{S_t} + 1 \tag{21}$$

where n_{d_t} is defined by Equation (16) provided that Q of the equation is the number of thermal neutrons per second emitted by the source.

C. Gamma Ray Scattering

The geometry for gamma ray scattering is the same as that for neutron scattering (Figure 1) and the development of an equation for monoenergetic gamma ray scattering is similar to the development of the equation for neutron scattering.

If it is assumed that no attenuation of the gamma rays occurs in the air, the gamma ray flux ϕ_γ which reaches the element of volume at P a distance r_1 from the source is

$$\phi_\gamma = \frac{S}{4 \pi r_1^2}$$

where S is the source strength in gamma rays per second.

The effective volume element at P is

$$dV = r_1 d\psi \, r_1 d\theta \, dr_1$$

The differential cross section $d\sigma/d\Omega$ for gamma ray scattering, which has units of per incident photon per electron per cm.^{2} per steradian, is the probability that a gamma ray will be scattered through an angle ϵ into the element of solid angle centered about ϵ. This cross section times the number of electrons n_e in a cubic cm. of the

scattering material times the volume element gives the probability of a photon being singly scattered through the angle ϵ into the element of solid angle centered about ϵ while within the volume element.

Consequently, the number of gamma rays n_γ scattered while within the volume element is the flux at the element times the probability of scattering within the element, or

$$dn_\gamma = \frac{S}{4\pi}\frac{d\sigma}{d\Omega} n_e d\theta \, d\Psi \, dr_1$$

The number of gamma rays $n_{s\gamma}$ which are scattered into the counting tube volume is the above equation multiplied by the solid angle subtended by the counting tube as seen from the volume element. This solid angle is given by Equation (4). To avoid the difficulties identical to those encountered in the neutron scattering equation development, the solid angle subtended by the counting tube was replaced by the average angle $\bar{\Omega}$. Equations (11), (12) and (13) are used to calculate $\bar{\Omega}$. Values of $\bar{\Omega}$ for the various geometries used in this investigation are plotted in Figure 2.

The number of gamma rays $n_{s\gamma}$ which are scattered into the counting tube volume is found by multiplying the above equation by this average angle. Thus,

$$dn_{s\gamma} = \frac{S\bar{\Omega}}{4\pi}\frac{d\sigma}{d\Omega} n_e d\theta \, d\Psi \, dr_1$$

The differential cross section $d\sigma/d\Omega$ which is a function of energy and the scattering angle is approximately constant for scattering angles greater than about 70 degrees. In this investigation and in similar setups with scattering material shells, the scattering angle is greater than 70 degrees except for shells with very small radii, thus, $d\sigma/d\Omega$ was assumed to be constant. The number of electrons per cubic cm. is a constant for a particular scattering material. These constants can be taken outside the integral and the equation for n_{s_γ} can be written

$$n_{s_\gamma} = \frac{S\,\bar{\Omega}\,n_e}{4\pi}\,\frac{d\sigma}{d\Omega}\int_{(r_1)_1}^{(r_1)_2}\int_{\psi_1}^{\psi_2}\int_{\theta_1}^{\theta_2} d\theta\, d\psi\, dr_1$$

where the subscripts 1 and 2 signify, respectively, minimum and maximum.

As in the neutron scattering equation development, the limits on r_1, ψ, and θ are

$$(r_1)_1 = \frac{r}{\sin\theta}$$

$$(r_1)_2 = \frac{r+t}{\sin\theta}$$

$$\psi_1 = 0$$

$$\psi_2 = 2\pi$$

$$\theta_1 = \cot^{-1}\frac{h_3}{r}$$

$$\theta_2 = \cot^{-1}\frac{h_1}{r}$$

In the latter limit, h_1 is considered positive if the bottom edge of the cylindrical shell is horizontally above the source and negative if the bottom edge is below the source.

Integrating and applying these limits gives the expression for the number of monoenergetic gamma rays per second that are singly scattered into the counting tube volume. This expression is

$$n_{s\gamma} = \frac{S\,\bar{\Omega}\,n_e t}{2}\,\frac{d\sigma}{d\Omega}\left[\ln\left(\sqrt{1+\left(\frac{h_1}{r}\right)^2}-\frac{h_1}{r}\right)-\ln\left(\sqrt{1+\left(\frac{h_3}{r}\right)^2}-\frac{h_3}{r}\right)\right]$$

The term within the brackets is M which was defined in the neutron scattering equation development. A plot of M versus β_b for various values of β_f is given in Figure 3. Placing M in the above equation

gives

$$n_{s_\gamma} = \frac{S\,\Omega\,n_e tH}{2}\,\frac{d\sigma}{d\Omega} \tag{22}$$

The ratios R_S and R_T were defined in the development of the equation for neutron scattering. R_S is n_s/n_d where n_d is the number of radiations that proceed directly from the source to the counting tube. This is given by Equation (16) with Q replaced by S. Thus, for gamma rays,

$$R_{S_\gamma} = \frac{\Omega\,n_e tH}{(1 - \cos\beta_d)}\,\frac{d\sigma}{d\Omega} \tag{23}$$

and

$$R_{T_\gamma} = R_{S_\gamma} + 1 \tag{24}$$

V. EXPERIMENTAL PROGRAM

A. Materials

The materials used in this investigation were 24ST and Alclad 24ST aluminum alloy, paraffin, cadmium, lead, plywood, borated sand, a neutron source, and a gamma ray source.

The aluminum alloy was purchased from the Iowa State College Instrument Shop, the paraffin and plywood were purchased from local concerns, and the cadmium in the form of 0.010 inch sheet was purchased from the Division Lead Company, Summit, Illinois. The lead and borated sand were available in the laboratory.

A polonium-beryllium neutron source was used. This source is contained in two right cylinders. The outer cylinder has external dimensions of 1.0 inch diameter and 1.25 inches height. The dimensions of the inner cylinder, within which the source is sealed, were estimated by comparison with dimensions given by Rausa (8) for the same type of source. Thus, the inner right cylinder was estimated to have internal dimensions of 0.50 inch diameter and 0.60 inch height.

The strength of this source on about June 9, 1953 was 3500 millicuries, therefore, the strength at the time of the experiment (May 1955) was approximately 114 millicuries. The neutron production from a source of this type is estimated at 2500 neutrons per second per millicurie so the flux from this source was approximately 2.85×10^5 neutrons per second. Rausa (8) stated that the suggested maximum permissible exposure to polonium-beryllium neutrons for a 40 hour week

is 34 neutrons per square cm. per second. Consequently, the tolerance distance in air for the source used here was about 10 inches.

Elliot and others (9) investigated the energy spectrum from a polonium-beryllium neutron source and found that the maximum neutron energy is about 12 Mev. Graphical integration of the spectrum they presented indicated that the neutrons emitted by this type source have an average energy of about 5 Mev.

The gamma ray source used was Co^{60}. This source had a strength of approximately 10 μ c. Calculations showed that a safe working distance in air for a 40 hour week with this source is slightly less than 2 inches. The Co^{60} was contained in a piece of Scotch tape that was rolled into the form of a right cylinder with dimensions of about 1/8 inch diameter and 3/8 inch height. This was sealed by adding other Scotch tape to it, thus, the source as used had external dimensions of about 1/4 inch diameter and 1 inch height.

B. Equipment

The major pieces of equipment used are shown in Figure 4. The shielding box has outside dimensions of 23 inches by 23 inches by 29 inches height and the inside chamber of the box has dimensions of 18 inches by 18 inches by 24 inches height. The walls of the box were made by sandwiching a 1½ inches thickness of paraffin between two ½ inch thicknesses of plywood. The front of the box was removable for access to the counting chamber which was lined with 0.010 inch cadmium sheet. This thickness of cadmium will capture approximately 90 per cent of the

Figure 4. Apparatus and experimental set-up

A --- Scaler

B --- Voltage regulator

C --- Detector and source suspension rig

D --- Detector and source in position

E --- Stand for holding cylindrical shells

F --- Cylindrical shells

G --- Shielding box with front removed

incident neutrons that have energies of 0.25 ev or less which were here defined as slow neutrons. The paraffin-plywood sandwich by moderating any incoming fast neutrons increases the probability of capturing them in the cadmium. A hole to accommodate the counting tube cable was drilled through the center of the top of the box. Two small eye-hooks were screwed into the top of the chamber. The fine cord (approximately 0.018 inch in diameter) that was used for suspending the detector and source was fastened to these hooks.

The 24ST and Alclad 24ST aluminum alloy was rolled into cylindrical shells by the Iowa State College Instrument Shop. Since smooth shells were desired, the longitudinal junction was not riveted or welded but simply held together with Scotch tape, except for two of the heavier gage shells. For these, due to excessive outward spring action, fine cord had to be used to hold the junction.

All of the seven different cylindrical shells used were 16 inches high. Three of these, rolled from 24ST aluminum alloy sheet, had a shell thickness of 0.025 inch and a radius of 3, 4.5, and 6 inches respectively; two, rolled from Alclad 24ST aluminum alloy sheet, had a shell thickness of 0.064 inch and a radius of 6 and 8 inches respectively; and two, also rolled from Alclad 24ST aluminum alloy sheet, had a shell thickness of 0.126 inch and a radius of 4.5 and 8 inches respectively.

For neutron counting, the counting circuit was composed of a B^{10} lined proportional counter connected directly to the amplifying circuit of an electronic scaler. The proportional counter was manufactured by

General Electric and has a cylindrical active volume of 1.25 inches in diameter by 8.0 inches in length.

A Model 200 scaler manufactured by the Radiation Instrument Development Laboratory was used. This model has a built-in amplifying circuit and is equipped with a discriminator, a gain control, a register, and a timer. The input voltage to the scaler was maintained at 115 volts by a "Stabiline" type IE5101 voltage regulator.

The operating characteristics of the neutron counting circuit were investigated thoroughly. With the discriminator set at 70 and the gain switch on F, a 25 volt plateau of 2.5 per cent slope was found in the voltage range centered about 675 volts. Thus the operating voltage, discriminator, and gain were set at these values for neutron counting.

A Tracerlab TGC8 Geiger tube and the above scaler were used to count gamma rays. This Geiger tube has a cylindrical active volume of 1.5 inches diameter and 2.375 inches length.

Additional equipment included a level, a plumb line, and scales.

C. Procedure

The procedures finally used for counting neutrons and gamma rays were the result of experimenting with various shielding arrangements until the most satisfactory arrangements that were possible with the equipment available were determined.

The shielding box, which was explicitly built for the neutron counting, did not prove satisfactory. It reduced the neutron background, both fast and slow, to practically zero, but with the source and

detector in the box, its scattering of source neutrons greatly overshadowed its value as a shield against fast and slow neutrons impinging on the outside of the box. With the source suspended 4 inches below the detector, the fast neutron count in the box was approximately 20 times the count outside the box and the slow neutron count was approximately tripled. Therefore, the neutron counting was done outside the box.

A few exploratory counts outside the box showed that the scattering from the air and the room was lower with the source suspended some distance above the floor rather than directly next to the floor. Thus, the experimental arrangement shown in Figure 4 resulted.

The shielding box, as expected, was found to be ineffective as a gamma ray shield. The shielding material available included 10 pieces of lead each with dimensions of about ½ inch by 8 inches by 16 inches, 23 pieces of lead each with dimensions of about 3/4 inch by 1 and 3/4 inches by 4 inches, and 2 boxes and 2 bags of borated sand averaging about 10 inches in thickness.

With the gamma ray source and detector suspended in the box, two of the larger pieces of lead were placed on the floor of the counting chamber to determine the effectiveness of the lead in reducing the gamma ray scattering caused by the air and the room. This arrangement did not noticeably reduce the scattering. In fact, with these two pieces of lead in position and all the remaining available lead and the borated sand placed next to the outside of the box, the count still was not noticeably reduced. Therefore, the gamma ray counting was done outside

[illegible]

[illegible]

[illegible]

[illegible]

the box, where a few exploratory counts showed that the scattering from the air and room could be materially reduced over similar scattering inside the box. These exploratory counts indicated that the distance the source and detector was placed above the floor of the room did not influence the scattering appreciably, and that the scattering was reduced to the minimum possible by suspending the source and detector just above the floor with all the available lead placed below them. The best arrangement was found to be 1½ inches by 16 inches by 16 inches of lead centered directly under the counter and source with the remaining four large pieces of lead placed flat on the floor one on each of the four sides of this central arrangement and with the 23 smaller pieces of lead placed in the spaces between these outer blocks.

The method of suspending the source and detector for gamma ray counting was similar to that shown in Figure 4 except, of course, the source and detector were suspended in a position closer to the floor.

All the neutron counts, with the exception of one background count and one other count made to determine the number of slow neutrons being scattered by the air and the room into the detector, were taken with the detector covered with 0.010 inch of cadmium. This thickness of cadmium will capture approximately 98 per cent of the incident neutrons that have energies of 0.25 ev or less. Since any neutron with an energy higher than this was considered to be a fast neutron, the counts taken with the detector covered were due to fast neutrons. Only fast neutron counts were taken because practically all the neutrons

emitted by a source of this type are fast neutrons.

Since the results of this investigation depended to a great extent on the correctness and duplication of geometrical arrangements, every effort was made to assure such conditions for both the neutron and gamma ray measurements. The procedure in each case was identical.

The counting tube was suspended by four pieces of fine cord (approximately 0.018 inch in diameter) which were fastened to four eye-hooks screwed into the upper side of the cross bar of the suspension apparatus. The cords were secured in a manner that would allow the distance between the detector and the cross bar to be either shortened or lengthened by simply turning the hooks in the proper direction. This method was also used to vertically align the counting tube. The distance h_4 between the top of the active volume of the counting tube and the lead blocks in the case of gamma ray counting or the stand for holding the cylindrical shells in the case of neutron counting was carefully measured with a measuring stick. The vertical alignment of the counting tube was checked with a level and also by sighting along a plumb line that was suspended behind the apparatus. The background counts were made with the counting tubes suspended in this position.

The source was suspended below the detector by a piece of fine cord which was fastened at each end to another piece of cord that was placed around the detector just above its bottom edge. The distance h_5 between the source and the bottom of the active volume of the detector was measured and then checked by measuring the distance from the source to the lead blocks in the case of gamma ray counting or the

stand for holding the cylindrical shells in the case of neutron counting. These distances were measured from the vertical mid-point of the source as estimated from the dimensions given previously. The centering of the source below the detector was checked by placing the level vertically along the detector so that it projected past the position of the source and then measuring the horizontal distance from the level to the source.

A gamma ray count and both a fast and slow neutron count were made with just the source and detector in position. These counts were made for each value of h_s used and, when corrected for the scattering caused by the air and room, they are the counts due to the radiation that proceeds directly from the source to the detector.

To determine the counts that are caused by the sum of the radiation that proceeds directly and that that is scattered into the detector by the aluminum alloy cylindrical shells, the shells were positioned around the source and detector. The center line of these shells had to coincide with the center line of the detector. This alignment was checked by measuring the distance from the detector wall to the shell at various positions around the periphery of the shell. Furthermore, the shells were checked with the level to determine their vertical alignment. When the neutron detector was covered with cadmium this method of measuring around the periphery of the shell could not be followed, therefore, the seven different cylindrical shells used were positioned with the neutron detector uncovered, suitable markings were made on a piece of heavy paper that was taped to the stand that supported the shells, and these markings were then used for positioning

the shells when the detector was covered.

This system of positioning introduced the possibility of undetected horizontal movement of the alignment paper, the stand, or the detector, or the possibility of the detector and source not remaining aligned with the true vertical. An attempt was made to eliminate these possibilities by making the apparatus concerned as secure as possible. Furthermore, to be sure that the geometry remained the same during the counts, the vertical alignment of the B^{10} tube was checked before it was covered and again after it was uncovered and after the counts were taken the markings on the piece of paper on the stand were checked by placing one of the cylindrical shells in the position indicated by the markings and measuring to determine if the shell was still centered about the detector and source. In all cases no horizontal movement was detected. Of course this did not exclude the possibility of compensating movements occurring, but such combinations were highly unlikely.

The counts determined by positioning each of the cylindrical shells about the source and the detector were corrected for the scattering caused by the air and room and the resulting count was that due to the sum of the radiation scattered into the detector by the shell and the radiation that proceeds directly from the source to the detector. No correction was made for the secondary effect of the room or air scattered radiation, which normally returned to the counting tube when the cylindrical shell was not in position, being scattered away from the detector by the cylindrical shell when it was in position.

VI. EXPERIMENTAL RESULTS AND DISCUSSION

A. Neutron Scattering

The experimental results for neutron scattering by the aluminum alloy cylindrical shells are listed in Table 1. The difference between the first two counting rates listed for both h_5 equal 4 inches and h_5 equal 3 inches is the counting rate due to slow neutrons. For 3 inches this difference is 27.3 ± 1.2 and for 4 inches it is 25.7 ± 1.1. Thus, the slow neutron counting rate remained practically constant with these two source positions, indicating that all the slow neutrons reaching the detector were the result of scattering by the air and room and that none of the slow neutrons are issued directly by the source.

The fast neutron counts given in Table 1 had to be corrected for the scattering due to the air and room. In making this correction it was assumed that the number of fast neutrons scattered by the air and room into the counting tube was not influenced by the aluminum cylindrical shells being present or by a small movement of the source.

The magnitude of this correction can be calculated from the formula

$$R_{T_F} = R_{D_F} + R_{W_F}$$

Table 1

Neutron counts

Cylindrical shell dimensions						
r (in.)	t (in.)	h_4 (in.)	h_5 (in.)	Counting time (minutes)	Net counting rate (R) (counts per minute)	Neutrons counted
	none		3	40	43.8 ± 1.1	fast and slow
	none		3	60	16.5 ± 0.5	fast
3	0.025	16	3	60	16.1 ± 0.5	fast
4.5	0.025	16	3	60	16.4 ± 0.5	fast
6	0.025	16	3	60	16.8 ± 0.5	fast
6	0.064	16	3	60	17.2 ± 0.5	fast
8	0.064	16	3	60	17.1 ± 0.5	fast
4.5	0.126	16	3	60	17.4 ± 0.6	fast
8	0.126	16	3	60	16.8 ± 0.5	fast
	none		4	40	35.4 ± 1.0	fast and slow
	none		4	60	9.7 ± 0.4	fast
3	0.025	16	4	60	10.1 ± 0.4	fast
4.5	0.025	16	4	60	10.3 ± 0.4	fast
6	0.025	16	4	60	9.5 ± 0.4	fast
6	0.064	16	4	60	9.9 ± 0.4	fast
8	0.064	16	4	60	9.9 ± 0.4	fast
4.5	0.126	16	4	60	11.7 ± 0.4	fast
8	0.126	16	4	60	10.2 ± 0.4	fast

where R_{T_F} is the total fast neutron counting rate

R_{D_F} is the fast neutron counting rate due to those neutrons that proceed directly from the source to the detector

R_{S_F} is the fast neutron counting rate due to those neutrons that are scattered by the air and the room into the detector.

As the distance h_5 between the source and detector is changed, R_{D_F} will vary according to Equation (16). This equation is based on the assumption of a point source. Calculations made by replacing the neutron source used here with a series of centrally located point sources showed that this assumption is still valid for values of h_5 equal to 3 inches and 4 inches.

The ratio of R_{D_F} at h_5 equal 3 inches to R_{D_F} at h_5 equal 4 inches is then

$$\frac{\left(R_{D_F}\right)_3}{\left(R_{D_F}\right)_4} = \frac{1 - \cos \beta_{d_3}}{1 - \cos \beta_{d_4}}$$

where $\cos \beta_d$ is calculated from the radius of the detector and the distance h_5. The radius of the detector used here is 0.625 inch, so that the above ratio is 1.75.

Now

$$\left(R_{D_F}\right)_3 = \left(R_{T_F}\right)_3 - R_{W_F}$$

and

$$\left(R_{D_F}\right)_4 = \left(R_{T_F}\right)_4 - R_{W_F}$$

Dividing the first of these equations by the latter, substituting for the ratio $\left(R_{D_F}\right)_3 / \left(R_{D_F}\right)_4$, and rearranging results in the equation

Table 2

Fast neutron counting rates corrected for air and room scattering and total neutron scattering ratios

Cylindrical shell dimensions r (in.)	t (in.)	h_5 (in.)	Net counting rate (R) (counts per minute)	$R - R_{W_F}$ (counts per minute)	R_T experimental	R_T theoretical
none		3	16.5±0.5	15.8±1.3		
3	0.025	3	16.1±0.5	15.4±1.3	0.975±0.115	1.028
4.5	0.025	3	16.4±0.5	15.7±1.3	0.995±0.116	1.013
6	0.025	3	16.8±0.5	16.1±1.3	1.020±0.116	1.008
6	0.064	3	17.2±0.5	16.5±1.3	1.044±0.119	1.020
8	0.064	3	17.1±0.5	16.4±1.3	1.038±0.119	1.010
4.5	0.126	3	17.4±0.6	16.7±1.3	1.057±0.120	1.067
8	0.126	3	16.8±0.5	16.1±1.3	1.020±0.116	1.020
none		4	9.7±0.4	9.0±1.3		
3	0.025	4	10.1±0.4	9.4±1.3	1.044±0.209	1.047
4.5	0.025	4	10.3±0.4	9.6±1.3	1.067±0.211	1.023
6	0.025	4	9.5±0.4	8.8±1.3	0.967±0.200	1.013
6	0.064	4	9.9±0.4	9.2±1.3	1.022±0.205	1.034
8	0.064	4	9.9±0.4	9.2±1.3	1.022±0.205	1.018
4.5	0.126	4	11.7±0.4	11.0±1.3	1.112±0.228	1.115
8	0.126	4	10.2±0.4	9.4±1.3	1.044±0.209	1.035

$$R_{W_F} = \frac{1.75\left(R_{T_F}\right)_4 - \left(R_{T_F}\right)_3}{0.75}$$

This equation, upon substituting the fast neutron counting rates without a cylindrical shell in position for the two values of h_5 used, gave a value of 0.7 ± 1.2 counts per minute for R_{W_F}. The fast neutron counting rates corrected for this scattering are given in Table 2. The value of h_4 is 16 inches for all the cylindrical shells, therefore,

it is not listed in this table.

The experimental total neutron scattering ratios R_T, as determined by dividing each corrected counting rate taken with a cylindrical shell in position by the corrected counting rate when no shell was in position, is also listed. The last column in Table 2 lists the theoretical values of R_T which were computed by using Equation (13).

Any comparison of the experimental results with the theoretical values of R_T was impossible due to the statistical deviations in the experimental values. This large statistical deviation is for the most part caused by the deviation in the counting rate due to the scattering from the air and the room. Every possible effort was made to reduce this unwanted scattering to a statistically acceptable level, however, these efforts were not successful.

B. Gamma Ray Scattering

The experimental results for gamma ray scattering by the aluminum alloy cylindrical shells are listed in Table 3. Since h_4 is 16 inches for all the shells it is not listed in the table.

The net counting rates listed in the last column of Table 3 had to be corrected for the scattering due to the air and room. This correction was made in a manner identical to that used for the correction to the neutron counting rates. The gamma ray source was much smaller in dimensions than the neutron source, thus the assumption of a point source, as is required to apply Equation (16) is valid.

Table 4

Gamma ray counting rates corrected for air and room scattering and total gamma ray scattering ratios

Cylindrical shell dimensions r (in.)	t (in.)	h_s (in.)	Net counting rate (N) (counts per minute)	$N - R_{W_\gamma}$ (counts per minute)	R_{T_γ} experimental	R_{T_γ} theoretical
none		4	4752 ± 31	3970 ± 51		
3	0.025	4	4823 ± 32	4041 ± 52	1.018 ± 0.019	1.010
4.5	0.025	4	4853 ± 32	4071 ± 52	1.025 ± 0.019	1.005
6	0.064	4	4798 ± 32	4016 ± 52	1.012 ± 0.018	1.007
4.5	0.126	4	4875 ± 32	4093 ± 52	1.031 ± 0.019	1.024
8	0.126	4	4851 ± 32	4069 ± 52	1.025 ± 0.019	1.007
none		6	2507 ± 17	1805 ± 44		
3	0.025	6	2605 ± 17	1903 ± 44	1.055 ± 0.036	1.023
4.5	0.025	6	2525 ± 17	1823 ± 44	1.010 ± 0.035	1.010
6	0.025	6	2530 ± 17	1828 ± 44	1.013 ± 0.035	1.006
6	0.064	6	2570 ± 17	1868 ± 44	1.035 ± 0.035	1.015
8	0.064	6	2517 ± 17	1815 ± 44	1.006 ± 0.035	1.008
4.5	0.126	6	2651 ± 17	1949 ± 44	1.080 ± 0.036	1.052
8	0.126	6	2563 ± 17	1861 ± 44	1.031 ± 0.035	1.016

It was assumed that this value of R_{W_γ} remained constant with or without a cylindrical shell positioned around the source and detector. The gamma ray counting rates corrected for R_{W_γ} are listed in Table 4. The experimentally determined total gamma ray scattering ratios are also listed. These ratios were calculated by dividing the corrected gamma ray counting rate with a cylindrical shell in position by the corrected counting rate when no shell was in position. The theoretical values of R_{T_γ}, calculated from Equation (24), are listed in the last

column of Table 4.

An examination of the experimental values of R_{T_γ} shows that in certain cases, they tend to support the theoretical values. However, the statistical deviations in the experimental values are too broad to make any positive comparison between them and the theoretical values. For instance, with the cylindrical shell of 3 inches radius and 0.025 inch shell thickness and with h_5 equal to 6 inches, the percentage variation between the theoretical and the experimental value as found from the equation,

$$\text{percentage variation} = \frac{(R_{T_\gamma})_{\text{experimental}} - (R_{T_\gamma})_{\text{theoretical}}}{(R_{T_\gamma})_{\text{theoretical}}} \times 100$$

is 3.12 ± 3.52 per cent.

As in the experimental results for neutron scattering, the predominant contribution to the large deviations was the statistical variation in the calculated counting rate due to the air and the room scattering. This was reduced to the lowest possible value with the equipment available, but as is evident it was not reduced enough.

C. General Discussion

It is believed that an experimental procedure which will give useful results can be devised for measuring the radiation scattered by aluminum alloy cylindrical shells.

In the case of neutron counting, a detector with a higher efficiency for counting fast neutrons or a stronger source or a combination of these two would increase the probability of securing useful results. For gamma ray counting, the taking of longer counts may improve the results. However, it is still a probability that the scattering caused by the air and the room would be the predominating factor in the statistical accuracy. If this is found to be true, another method of experimentally determining the scattering caused by the cylindrical shells would be desirable.

In any room, the scattering caused by the air and the room is mainly due to the latter. Thus, the logical conclusion is to eliminate the room. This can be done by suspending the source, detector, and cylindrical shell from, say, a guide wire of a radio tower or some other similar structure as was done by Glasgow (1). If the experimental system is some distance above the ground and far enough away from the tower or other structure, the system is essentially in an infinite air medium and the only extraneous scatter would be from the air.

As a further refinement, the equations developed in this investigation for radiation scattering could be modified to include the scattering caused by the air. Glasgow (1) gave an equation for scattering of neutrons in an infinite air medium and Plesset and Cohen (5) presented an equation for gamma ray scattering by an infinite medium.

VII. CONCLUSIONS

The experimental results, although tending to support the theoretical gamma ray scattering calculations, did not prove or disprove the analytical investigation results.

A more elaborate experimental system and procedure and a more efficient fast neutron detector or a stronger source or both would probably be needed to secure useful experimental results.

The scattering of neutrons and gamma rays by the air and the room was the predominant factor in producing the large statistical deviations in the corrected counting rates. These statistical deviations were the major cause of the poor results, although the low neutron counting rates were a contributing factor.

VIII. LITERATURE CITED

1. Glasgow, D. W. Neutron scattering from the walls and air of a laboratory. Richland, Washington. Hanford Atomic Products Operation HW-32086. June 9, 1954.

2. Plesset, M. S. Scattering of gamma rays and neutrons. Douglas Aircraft Company, Project Rand Report RAD-196. April 29, 1947. (Original not available for examination; abstracted in Nuclear Science Abstracts. 1: 522. 1948.)

3. Plesset, M. S. and others. Effect of source and shadow shield geometry on the scattering of gamma rays. Douglas Aircraft Company, Project Rand Report RAD-236. February 26, 1948. (Original not available for examination; abstracted in Nuclear Science Abstracts. 1: 436. 1948.)

4. Hine, Gerald J. and McCall, Richard C. Gamma-ray backscattering. Nucleonics. 12: 27-30. April, 1954.

5. Plesset, M. S. and Cohen, S. T. Scattering and absorption of gamma-rays. Journal of Applied Physics. 22: 350-357. 1951.

6. Alco aluminum and its alloys. Pittsburg, Pa., Aluminum Company of America. 1947.

7. Glasstone, Samuel and Edlund, Milton C. The elements of nuclear reactor theory. New York, D. Van Nostrand Company, Inc. 1952.

8. Rausa, Gerald J. Gamma dose rate from a Po-Be source. Nucleonics. 12: 62. February, 1954.

9. Elliot, J. O. and others. Energy spectrum of neutrons from Po-Be. Physical Review. 93: 1348-1349. 1954.

IX. ACKNOWLEDGMENTS

My thanks to Dr. Glenn Murphy for his original suggestion of this problem, for the guidance and help which he gave during our association at Iowa State College, and for the loan of certain apparatus used in the experimental part of this investigation.

I would also like to express my appreciation to Dr. A. F. Voigt for his loan of certain apparatus and the sources used in this investigation.

My work at Iowa State College was the third and final year of the Aeronautical Engineering Curriculum of the United States Naval Postgraduate School, Monterey, California, therefore, I would like to express my appreciation to the Naval Postgraduate School for making my work at Iowa State College possible.

X. APPENDIX

A. Sample Analytical Computations

The average values of the solid angle $\bar{\Omega}$ subtended by the detector were calculated by using Equations (11), (12), and (13).

The neutron detector used in this investigation has an active volume in the shape of a right cylinder with dimensions of 1.25 inches diameter and 8 inches height. Thus, for this detector the value of h_2 is 8 inches, a is 0.625 inches and d which is equal to $(\pi a)/4$ is 0.491 inches. For this calculation a cylindrical shell with a 3 inch radius and 16 inch height was used. The values assigned to h were 0, 1, 2, 3,...........14, 15, 16 inches. Equation (11) was used with values of h from 0 through 8 inches and Equation (12) was used with values of h from 9 through 16 inches. For h equal 0 inches, substitution into Equation (11) gave Ω_0 equal 0.392 and, for h equal 1 inch, Ω_1 equal 0.539.

The value of Ω was thus determined for each of the 17 values assigned to h and these Ω's were then summed using Equation (13). For this particular cylindrical shell and detector, $\bar{\Omega}$ was found to be 0.367 steradians. This value is plotted on the upper curve of Figure 2 at r/h_4 equal 0.1875.

The factor N which is plotted in Figure 3 was calculated using the equation

$$H = \ln \left[\left(\frac{1 - \sin \beta_b}{\cos \beta_b} \right) \left(\frac{\cos \beta_f}{1 - \sin \beta_f} \right) \right]$$

For β_b equal -30 degrees and β_f equal 70 degrees, substitution gave H equal 2.285.

The theoretical values of R_T, the total neutron scattering ratio, are calculated using Equation (18). For this sample computation a value of 3 inches for h_5 and the cylindrical shell with 6 inches radius, 0.064 inch shell thickness and 16 inches height was selected. The value of $\bar{\Omega}$ for this geometry and the neutron detector used was taken from Figure 2. This value is 0.159 steradians. The backward angle β_b for this geometry is -39.8 degrees and the forward angle β_f is 61.4 degrees, thus the value of H as given in Figure 3 is 2.12. The mean free path for scattering, λ_s was assumed to be constant at the thermal value throughout the energy spectrum of neutrons emitted by this source. For the cladding which is 5 per cent of the total thickness of the sheet, λ_s is 11.76 cm. and for the 24ST aluminum λ_s is 10.6 cm. Thus, λ_s for the Alclad 24ST is 0.05 times 11.76 cm. plus 0.95 times 10.60 cm. which is 10.66 cm. The detector angle β_d for this detector and geometry is 11.75 degrees. Substituting these values into Equation (18) gave R_T equal 1.034.

Equation (24) was used to calculate the theoretical values of $R_{1\gamma}$,

the total gamma ray scattering ratio. For this sample calculation, a value of 4 inches for h_5 and the cylindrical shell with 6 inch radius, 0.064 inch shell thickness and 16 inches height was selected. The Geiger tube has a cylindrical active volume of 1.5 inches diameter by 2.375 inches length. The value of $\bar{\Omega}$ for this geometry, as taken from Figure 2, is 0.052 steradians.

Assuming that the amount of impurities present is one-half of the maxima, n_e, the number of electrons per cubic cm., for the 24ST aluminum alloy was calculated to be 8.02×10^{23} and for the cladding, 7.93×10^{23}. Thus, the weighted value of n_e is 0.05 times 7.93×10^{23} plus 0.95 times 8.02×10^{23} which is 8.02×10^{23}.

The backward angle for this geometry is -58.0 degrees and the forward angle is 46.75 degrees, thus the value of H as given in Figure 3 is 2.17. The detector angle for this geometry is 10.6 degrees.

The differential cross section $d\sigma/d\Omega$ for gamma ray scattering is a function of both the gamma ray energy and the angle of scattering. However, it was previously assumed that a constant value could be used for angles of scattering greater than about 70 degrees. Plesset and Cohen (5) presented a plot of $d\sigma/d\Omega$ for various gamma ray energies and angles of scattering. For 1.02 Mev gamma rays, the average value of $d\sigma/d\Omega$ for scattering angles greater than 70 degrees is 0.89×10^{-26} per electron per square cm. and for 1.53 Mev gamma rays it is 0.64×10^{-26} per electron per square cm.

Every disintegration of a Co^{60} nucleus results in the emission of a cascade of two gamma rays, the first with an energy of 1.17 Mev and

the second with an energy of 1.33 Mev. By using straight line interpolation between the two values of $d\sigma/d\Omega$ given above, $d\sigma/d\Omega$ for the 1.17 Mev gamma rays was found to be 0.82×10^{-26} per electron per square cm. and for the 1.33 Mev gamma rays it was evaluated as 0.74×10^{-26} per electron per square cm. Since the number of gamma rays issued by the source are equal for each of the two energies, the final value of $d\sigma/d\Omega$ was found by multiplying each of the two values of $d\sigma/d\Omega$ by 0.5 and adding. Thus $d\sigma/d\Omega$ used in the equation for $R_{T\gamma}$ is 0.78×10^{-26} per electron per square cm.

Substituting the quantities evaluated above gave a value of 1.0067 for $R_{T\gamma}$.

thesN47
Similitude considerations in neutron and
3 2768 001 89957 8
DUDLEY KNOX LIBRARY